



## OPEN Predicting lymph node metastasis in papillary thyroid carcinoma with Hashimoto's thyroiditis using regression and network analysis

Lirong Wang<sup>1</sup>, Peng Cheng<sup>4</sup>, Lian Zhu<sup>1</sup>, Hailong Tan<sup>1</sup>, Bo Wei<sup>1</sup>, Ning Li<sup>1</sup>, Neng Tang<sup>1</sup> & Shi Chang<sup>1,2,3,5</sup>✉

The comprehensive study of the relationship between lymph node metastasis (LNM) and its associated factors in patients with concurrent papillary thyroid carcinoma (PTC) and Hashimoto's thyroiditis (HT) remains insufficient. Building upon the initial investigation of factors associated with LNM in patients with concurrent PTC and HT, we further analyzed the complex relationships between different severity indicators of LNM and these associated factors. This study included patients confirmed PTC with HT who underwent total thyroidectomy at Xiangya Hospital, from January 2020 to December 2021. A total of 271 patients from 2020 were used as the training set, and 300 patients from 2021 as the validation set. Univariate analysis and regression modeling were used to identify key factors associated with LNM. Model reliability was assessed using the area under the receiver operating characteristic curve (AUC). Network analysis was employed to explore associations between LNM severity and its related factors. The regression model indicated that age, calcification, free triiodothyronine (FT3), and tumor maximum diameter (TMD) are independent factors for LNM. The severity model showed free thyroxine (FT4) and hemoglobin (Hb) are independent protective factors for the region and quantity of LNM, respectively, while TMD is an independent risk factor for both. Network analysis revealed TMD has a closer relationship with LNM severity compared to other associated factors. This study innovatively combined regression models and network analysis to investigate factors related to LNM in patients with PTC and HT, providing a theoretical basis for predicting preoperative LNM in future clinical practice.

### Highlights

- **Innovative Methods:** First to combine regression models and network analysis for LNM study.
- **Risk Factor Identification:** Identified 4 independent risk factors for LNM in PTC with HT.
- **Detailed Subgroup Analysis:** Uncovered specific risk factors for LNM severity and regional spread.

**Keywords** Papillary thyroid carcinoma (PTC), Hashimoto's Thyroiditis (HT), Lymph Node Metastasis (LNM), Biochemical markers, Regression modeling, Network Analysis

Over the past 30 years, the incidence of thyroid cancer (TC) has rapidly increased across various populations worldwide, with papillary thyroid carcinoma (PTC) being the most prevalent subtype, accounting for approximately 80–90%<sup>1–3</sup>. Despite being classified as a low-grade malignancy, about 30–80% of PTC patients present with lymph node metastasis (LNM), which is strongly associated with higher rates of locoregional recurrence<sup>4,5</sup>.

Hashimoto's thyroiditis (HT) is the most common autoimmune thyroid disease and the most frequent benign comorbidity in PTC patients (10–58% of PTC patients also have HT)<sup>6–10</sup>. Although some studies suggest that

<sup>1</sup>Division of Thyroid Surgery, General Surgery Department, Xiangya Hospital, Central South University, No.87 Xiangya Road, Changsha 410008, Hunan, China. <sup>2</sup>Hunan Provincial Clinical Medical Research Centre for Thyroid Diseases, No.87 Xiangya Road, Changsha 410008, Hunan, China. <sup>3</sup>Hunan Engineering Research Center for Thyroid and Related Diseases Diagnosis and Treatment Technology, No.87 Xiangya Road, Changsha 410008, Hunan, China. <sup>4</sup>Department of Psychiatry, National Center for Mental Disorders, National Clinical Research Center for Mental Disorders, The Second Xiangya Hospital of Central South University, Changsha 410011, Hunan, China. <sup>5</sup>Department of General Surgery, Xiangya Hospital Central South University, 87 Xiangya Road, Changsha 410008, China. ✉email: changshi@csu.edu.cn

HT may have a protective role against LNM in PTC patients<sup>11–14</sup>, there remains a considerable risk of LNM (28–62%) in patients with concurrent PTC and HT<sup>7,15,16</sup>. The presence of LNM, the number of LNM, and the regions affected significantly influence the surgical approach and prognosis for PTC patients. Current research suggests that the factors influencing LNM in PTC patients with concurrent HT may differ from those in PTC patients without HT<sup>17–19</sup>. While LNM in PTC-only patients has been well-studied, there remains a gap in understanding the risk factors for LNM in patients with both HT and PTC, primarily due to incomplete inclusion of relevant variables and the absence of comprehensive criteria for assessing LNM. Additionally, reactive hyperplasia commonly observed in cervical lymph nodes, particularly in the central compartment, complicates the preoperative radiological evaluation of metastasis in patients with both PTC and HT<sup>8,20</sup>. Therefore, investigating the factors contributing to LNM and constructing predictive models is crucial for improving the accuracy of preoperative diagnosis in this patient population.

Moreover, while the majority of prior clinical studies have employed group-based differential testing methods to investigate the potential risk factors for LNM, the experimental design based on specific indicators has limited capacity to exclude the influence of potential confounding factors<sup>21</sup>. Furthermore, these studies have failed to conduct an in-depth exploration of the mutual influences between the key outcome variable and the risk factors. Therefore, building upon the risk factors for LNM in patients with HT and PTC revealed by regression models, this study aims to further investigate the intricate interplay between the severity of LNM and the associated risk factors among patients with concurrent HT and PTC who exhibit LNM, through the employment of robust data-driven analytical methodologies. The emerging paradigm of symptom network analysis presents an opportune avenue to address this inquiry.

Network analysis is a data-driven analytical approach grounded in mathematical graph theory, which has been widely utilized in recent years to conduct in-depth investigations of the interrelationships among different omics data. In symptom network analysis, variables are represented as nodes within the network, and the correlations between variables are depicted as edges. Algorithms such as the extended Bayesian information criterion (EBIC) and the least absolute shrinkage and selection operator (LASSO) are employed to eliminate spurious correlations within the network, thereby controlling for the potential influence of confounding factors on the associations between nodes<sup>22,23</sup>. Moreover, symptom network analysis not only allows for the visualization of complex interrelationships among variables but also facilitates the detection of clustering communities within the network, further elucidating the clustering preferences among variables. By leveraging the novel capabilities of symptom network analysis and other data-driven techniques, we aim to unravel the intricate interdependencies between the extent of LNM and the pertinent associated factors in the clinical cohort.

In summary, within this study, we systematically gathered data encompassing age, gender, preoperative serum autoantibody levels, tumor ultrasound characteristics, and the presence of the BRAF<sup>V600E</sup> mutation. The primary objective was to elucidate the integrated clinical and pathological features of PTC combined with HT and to explore their correlation with LNM. Furthermore, we employed emerging network analysis methods to further investigate the complex relationships between the severity of LNM and its associated factors.

## Materials and methods

### Participants and study design

This study received approval from the Ethics Review Committee of Xiangya Hospital, Central South University (202211733). All procedures were conducted in accordance with relevant guidelines and regulations, including the Declaration of Helsinki. Written informed consent was obtained at the time of surgery for general use of clinical information in future studies.

The study cohort comprised individuals who underwent total thyroidectomy and ipsilateral or bilateral central LN dissection and other necessary lateral neck LN dissection procedures at Xiangya Hospital, Central South University, spanning from January 2020 to December 2021. Data from the 2020 cohort were used as the training set for constructing the predictive model, while data from the 2021 cohort served as the validation set. Inclusion criteria encompassed pathologically confirmed PTC concomitant with HT. Exclusion criteria were applied to (i) individuals with mixed thyroid carcinomas, (ii) PTC combined with other head and cervical malignancies or inflammatory diseases, (iii) a history of cervical surgery, or (iv) incomplete clinical information. Ultimately, 271 patients in 2020 and 300 in 2021 with both PTC and HT were included in this investigation (Fig. 1).

### Variable definition and evaluation

The clinicopathological characteristics including age, gender, results of thyroid function tests [free triiodothyronine (FT3); free thyroxine (FT4); thyroid-stimulating hormone (TSH)], preoperative level of antithyroglobulin antibodies (TgAb) and thyroid peroxidase antibody (TPOAb), thyroglobulin (TG), parathyroid hormone (PTH), complete blood count, serum Ca<sup>2+</sup> levels, BRAF<sup>V600E</sup> mutation. Capsular invasion, extrathyroidal extension and vascular invasion were determined from postoperative pathological findings. The reference TgAb and TPOAb ranges were less than 115 IU/mL and less than 34 IU/mL, respectively.

Ultrasound characteristics of thyroid nodules such as tumor maximum diameter (TMD), sum of tumor diameters, multifocality, tumor location (left, right, isthmus, and bilateral of the thyroid gland), aspect ratio (the anteroposterior dimension/the transverse diameter:  $\leq 1$  or  $> 1$ ) and calcification. To ensure the reliability of ultrasound assessments, all examinations were performed by experienced thyroid radiologists utilizing high-resolution ultrasound systems, with reports subsequently reviewed and verified by both junior and senior radiologists. Additionally, preoperative evaluations commonly included follow-up imaging at multiple time points, allowing for comparison of findings to enhance diagnostic accuracy and reliability.

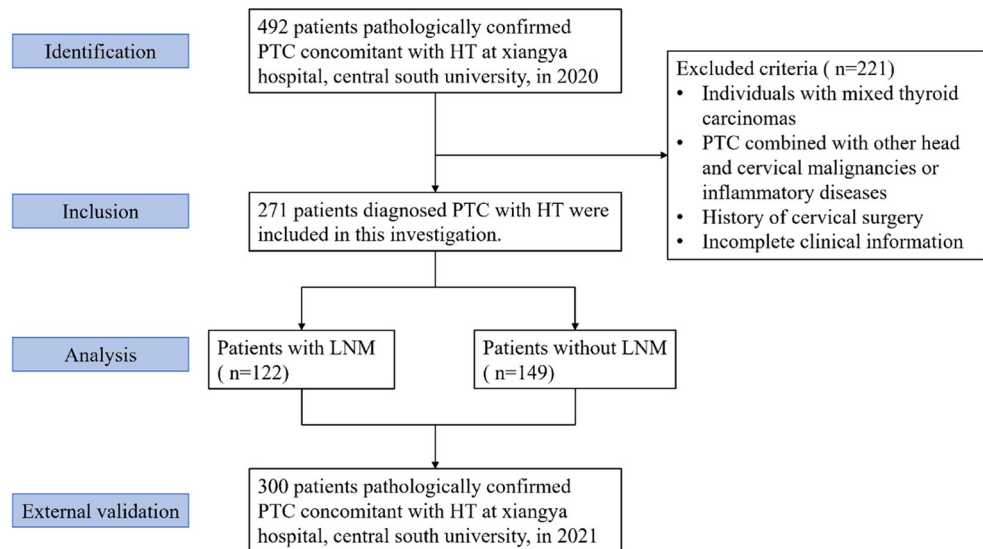


**Fig. 1.** The strobe flow of the inclusion and exclusion criteria for the study.

HT coexistence was ascertained through postoperative sectioning and examination of paraffin-embedded thyroid tissue specimens. A positive determination entailed the identification of diffuse lymphocytic and plasma cell infiltrate, oxyphilic cells, the development of lymphoid follicles, and the presence of reactive germinal centers.

LN status was defined based on post-operation pathological results. The LNM status encompasses (1) the presence of LNM (metastasis or non-metastasis) for all patients, (2) the regions of LNM [central lymph node metastasis (CLNM) or lateral lymph node metastasis (LLNM)] and (3) the quantity of LNM (According to the 2015 ATA Guidelines for Differentiated TC recurrence risk stratification<sup>4</sup>, 1–5 nodes are categorized as few LNM and > 5 nodes as numerous LNM) for patients diagnosed with LNM. Patients were staged according to the eighth edition of the International Union Against Cancer/American Joint Committee on Cancer TNM staging system<sup>24</sup>. All acquired surgical specimens were examined by two or more board-certified pathologists from the department of pathology of the Xiangya Hospital, Central South University.

### Descriptive and regression analysis

Continuous variables were expressed as mean  $\pm$  standard deviation (SD), while categorical variables were presented as frequencies and percentages (%). Clinicopathologic characteristics were compared among groups using the t-test for continuous variables and the Pearson  $\chi^2$  test (for expected values > 5) or Fisher's exact  $\chi^2$  test (for expected values  $\leq$  5) for categorical variables. Stepwise logistic regression was used to identify independent factors associated with LNM: Initially, an analysis was conducted across all patients to determine the factors that influence LNM in individuals with concurrent HT and PTC. Subsequently, for patients diagnosed with LNM, the investigation was focused on identifying the factors that affect the quantity and regions of lymph node metastases in this specific patient cohort. A two-tailed P-value of < 0.05 was considered statistically significant for variable inclusion. Receiver operating characteristic (ROC) curves were constructed, and area under the curve (AUC) values were calculated to assess the predictive performance of the regression model, with higher AUC values indicating better predictive accuracy.

### Network analysis

#### Network estimation and visualization

The severity of LNM (regions and quantity of metastases) and their independent associated factors were utilized in the network construction to explore the complex interrelationships among them. This study employed the Least Absolute Shrinkage and Selection Operator (LASSO) combined with the Extended Bayesian Information Criterion (EBIC) to eliminate spurious correlations among variables, thereby making the network easily analyzable and comprehensible. The detailed process and parameter settings for the network analysis can be found in Method S1.

#### Community clustering analysis

The Walktrap algorithm was utilized in community clustering analysis to detect the clustering characteristics of different nodes within the network, thereby determining the bias of various independent associated factors towards different severity indicators of LN metastasis. The Walktrap algorithm is based on the concept of random walks<sup>25</sup>, identifying communities within the network model through the simulation of random walks. In this study, the *igraph* R package was employed to perform the aforementioned steps.

### Network accuracy and stability

To ensure the reliability of edge in the network, this study evaluated both the accuracy of individual edges and the differences between pairwise edge weights<sup>26</sup>. A non-parametric bootstrap method was employed to construct 95% confidence intervals, which were used to assess edge weight accuracy, with narrower intervals indicating higher reliability. Additionally, to determine statistical differences between pairwise edge weights, a bootstrap difference test was conducted using confidence intervals. The presence of statistically significant differences between compared edges was inferred if the confidence intervals did not contain zero for any pairwise comparisons. Procedures above were completed with the *bootnet* (version 1.5) R package.

## Results

### Descriptive statistics

A total of 271 patients with pathologically confirmed PTC and concurrent HT were included in this study, comprising 233 women and 38 men (female-to-male ratio: 6.1:1). LNM was found in 122 (45.0%) patients, with 29 patients exhibiting LLNM. In this study, 238 patients (78.7%) were younger than 55 years, and 157 (57.9%) patients had a TMD  $\leq 1$  cm. Additionally, this study indicated a significantly high prevalence of BRAFV600E gene mutations and calcification in this patient cohort, at 78.7% (192/244) and 73.8% (200/271) respectively (Table 1).

### Univariate analysis

#### *The presence or absence of lymph node metastasis*

Univariate analysis was conducted among 271 patients in 2020 with concurrent HT and PTC, aiming to preliminarily explore the clinicopathological factors affecting the occurrence of LNM within this cohort. We observed that LNM was significantly correlated with age ( $P < 0.001$ ) with a notably greater number of patients under the age of 55 in the group exhibiting LNM compared to the group without (92.6% VS 83.9%,  $P = 0.029$ ). And LNM in PTC patients with HT was significantly correlated with FT3 ( $P = 0.01$ ) and preoperative level of TgAb ( $P = 0.039$ ). Certain ultrasound characteristics, including TMD ( $P < 0.001$ ), sum of tumor diameters ( $P < 0.001$ ), and calcification ( $P < 0.001$ ), were also significantly associated with LNM. Meanwhile, while there was a slightly higher prevalence of BRAF gene mutation positivity among patients with LNM (79.7% vs. 77.9%), this discrepancy did not reach statistical significance ( $P = 0.734$ ). This suggests that BRAF gene mutation may not exert an influence on LNM in patients with concurrent HT and PTC (Table 1).

#### *The quantity and regions of lymph node metastases*

Table 2 illustrates the correlations between the quantity of LNM and clinicopathological characteristics of PTC patients with HT, comprising a total of 122 patients diagnosed with LNM. A significant association was found between tumor diameter and the quantity of LNM, with both TMD ( $P = 0.003$ ) and sum of tumor diameters ( $P = 0.013$ ) showing statistical significance. Conversely, several variables—FT4 levels ( $P = 0.037$ ), Erythrocyte count (RBC) levels ( $P = 0.031$ ), hemoglobin (Hb) levels ( $P = 0.027$ ), serum  $\text{Ca}^{2+}$  levels ( $P = 0.033$ ), capsular invasion ( $P = 0.041$ )—previously lacking significant correlation with LNM in Table 1, demonstrated statistical significance. Of interest, there was no significant correlation between age and quantity of LNM in this cohort.

As demonstrated in Table 2, Significant differences were observed in the TMD ( $P = 0.031$ ), sum of tumor diameters ( $P = 0.026$ ), FT4 levels ( $P = 0.047$ ), PTH ( $P = 0.020$ ), and serum  $\text{Ca}^{2+}$  ( $P = 0.049$ ) among groups divided by regions of LNM.

### Multivariate logistic regression analyses

#### *Multivariate logistic regression analyses in all patients with PTC and HT*

Among all the PTC patients with HT, we selected statistically significant indicators from Table 1 for logistic regression analysis. As shown in Table 3, the regression results for following indicators were statistically significant. The association between age and LNM is significantly negative ( $p < 0.001$ ). With each additional year of age, there is a 5% reduction in the likelihood of LNM (odds ratio [OR] = 0.950). Elevated serum FT3 levels ( $P = 0.039$ , OR = 1.448), increased TMD ( $P = 0.049$ , OR = 1.635) and calcification ( $P = 0.024$ , OR = 2.167) are identified as independent risk factors for LNM. Subsequently, ROC curves were generated for each indicator and the overall model, with the overall model achieving an area under the curve (AUC) of 0.769, indicating good predictive accuracy (Fig. 2A). The cut-off values for age, maximum tumor diameter, and FT3 were 47.5 years, 1.15 cm, and 4.825 pmol/L, respectively. Additional data from the ROC curve analysis, including positive predictive value (PPV), negative predictive value (NPV), and accuracy, are provided in Table S1.

#### *Multivariate logistic regression analyses in patients diagnosed with lymph node metastasis*

Based on Table 2, we selected statistically significant variables from each of the two groups for logistic regression analysis. Table 3 presents the logistic regression results for patients diagnosed with LNM. In assessing the factors influencing the quantity of LNM, increased TMD ( $P = 0.010$ , OR = 1.796) was identified as an independent risk factor for extensive LNM in patients with PTC and HT. Conversely, elevated hemoglobin (Hb) levels ( $P = 0.029$ , OR = 0.967) were found to be a protective factor. For regions of LNM, TMD ( $P = 0.010$ , OR = 1.856) emerged as an independent risk factor for LLNM. Interestingly, elevated FT4 levels ( $P = 0.008$ , OR = 0.747) were identified as an independent protective factor against metastasis from the central to the lateral lymph node region. The ROC curves for the two models, shown in Fig. 2B-C, had AUCs of 0.709 and 0.665, respectively, indicating acceptable model reliability. Further ROC curve data, including cut-off values, PPV, NPV, and accuracy, are provided in Table S1.

Category	Total, n (%)	Metastasis, n (%)	Non-metastasis, n (%)	P
No. of patients	271	122 (45)	149 (55)	
CLNM		93 (76.2)		
LLNM		29 (23.8)		
1–5 LNM		91 (74.6)		
> 5 LNM		31 (25.4)		
<b>Age (mean ± SD, years)</b>	41.72 ± 11.02	38.22 ± 10.44	44.58 ± 10.68	<0.001*
<55	238 (87.8)	113 (92.6)	125 (83.9)	0.029*
≥ 55	33 (12.2)	9 (7.4)	24 (16.1)	
<b>Gender</b>				
Male	38 (14)	17 (13.9)	21 (14.1)	0.970
Female	233 (86)	105 (86.1)	128 (85.9)	
<b>BRAF V600E mutation</b>				
Yes	192 (78.7)	90 (79.6)	102 (77.9)	0.734
No	52 (21.3)	23 (20.4)	29 (22.1)	
<b>TMD (mean ± SD, cm)</b>	1.21 ± 0.78	1.47 ± 0.93	0.99 ± 0.56	<0.001*
≤ 1 cm	157 (57.9)	52 (42.6)	105 (70.5)	<0.001*
> 1 cm	114 (42.1)	70 (57.4)	44 (29.5)	
<b>Sum of tumor diameters (mean ± SD, cm)</b>	1.46 ± 0.95	1.71 ± 1.03	1.25 ± 0.82	<0.001*
<b>Multifocality</b>				
Yes	89 (32.8)	42 (34.4)	47 (31.5)	0.615
No	182 (67.2)	80 (65.6)	102 (68.5)	
<b>Tumor location (L/R/I/B)</b>				
Left	107 (39.5)	48 (39.3)	59 (39.6)	0.512
Right	105 (38.7)	47 (38.5)	58 (38.9)	
Isthmus	6 (2.2)	1 (0.8)	5 (3.4)	
Bilateral	53 (19.6)	26 (21.3)	27 (18.1)	
<b>Calcification</b>				
Yes	200 (73.8)	105 (86.1)	95 (63.8)	<0.001*
No	71 (26.2)	17 (13.9)	54 (36.2)	
<b>Capsular invasion</b>				
Yes	51 (18.8)	24 (19.7)	27 (18.1)	0.745
No	220 (81.2)	98 (80.3)	122 (81.9)	
<b>Extrathyroidal extension</b>				
Yes	6 (2.2)	4 (3.3)	2 (1.3)	0.414
No	265 (97.8)	118 (96.7)	147 (98.7)	
<b>Aspect ratio</b>				
≤ 1	97 (35.8)	36 (29.5)	61 (40.9)	0.051
> 1	174 (64.2)	86 (70.5)	88 (59.1)	
<b>Vascular invasion</b>				
Yes	10 (3.7)	6 (4.9)	4 (2.7)	0.353
No	261 (96.3)	116 (95.1)	145 (97.3)	
<b>TG (mean ± SD, ng/ml)</b>	18.58 ± 55.16	14.69 ± 50.10	21.75 ± 58.95	
<b>TgAb (mean ± SD, IU/mL)</b>	593.33 ± 912.61	690.00 ± 1031.81	515.21 ± 798.64	0.122
Normal	84(31)	30(24.6)	54(36.2)	0.039*
High	187(69)	92(75.4)	95(63.8)	
<b>TPOAb (mean ± SD, IU/mL)</b>	181.61 ± 192.80	184.97 ± 203.70	178.91 ± 184.27	0.800
Normal	95(35.1)	44(36.1)	51(34.2)	0.752
High	176(64.9)	78(63.9)	98(65.8)	
<b>FT3 (mean ± SD, pmol/L)</b>	4.89 ± 0.79	5.02 ± 0.74	4.78 ± 0.81	0.010*
<b>FT4 (mean ± SD, pmol/L)</b>	16.43 ± 3.07	16.67 ± 2.99	16.23 ± 3.14	0.246
<b>TSH (mean ± SD, mIU/L)</b>	2.85 ± 1.96	2.64 ± 1.92	3.03 ± 1.99	0.102
<b>PTH (mean ± SD, pg/ml)</b>	41.86 ± 36.95	37.88 ± 16.35	45.06 ± 47.30	0.132
<b>Leukocyte count (mean ± SD, 10<sup>9</sup>/L)</b>	5.78 ± 1.40	5.83 ± 1.39	5.73 ± 1.42	0.578
<b>Erythrocyte count (mean ± SD, 10<sup>12</sup>/L)</b>	4.87 ± 8.02	4.41 ± 0.51	5.26 ± 10.83	0.389
<b>Hemoglobin (mean ± SD, g/L)</b>	129.59 ± 15.79	129.61 ± 14.86	129.58 ± 16.57	0.990
Continued				
<b>Platelet count (mean ± SD, 10<sup>9</sup>/L)</b>	215.27 ± 58.83	214.19 ± 56.47	216.17 ± 60.89	0.783

Category	Total, n (%)	Metastasis, n (%)	Non-metastasis, n (%)	P
Vitamin D3 (mean ± SD, nmol/L)	20.48 ± 7.86	20.57 ± 8.10	20.39 ± 7.67	0.881
Serum Ca <sup>2+</sup> (mean ± SD, mmol/L)	2.32 ± 0.15	2.32 ± 0.12	2.32 ± 0.17	0.954

**Table 1.** Correlations between LNM and clinicopathological characteristics of patients with concurrent PTC and HT. Note: Abbreviations: LNM, lymph node metastasis; CLNM, central lymph node metastasis; LLNM, lateral lymph node metastasis; TMD, tumor maximum diameter; Tumor location (L/R/I/B), tumor location (left/right/isthmus/bilateral); TG, thyroglobulin; TgAb, antithyroglobulin antibodies; TPOAb, thyroid peroxidase antibody; FT3, free triiodothyronine; FT4, free thyroxine; TSH, thyroid-stimulating hormone; PTH, parathyroid hormone. \* Means  $P < 0.05$ .

#### External validation of the predictive model

The ROC curves from the external validation of three predictive models for LNM in patients with HT and PTC are displayed in Fig. 3. The AUC values for the models were 0.765, 0.709, and 0.607, respectively. Although Model 3 exhibited a decline in predictive accuracy for regions of LNM, the overall performance of the first two models, especially Model 1, suggests robust clinical utility. Additional clinicopathological information for the validation cohort can be found in Table S2.

#### Network of lymph node metastasis severity and associated factors

Based on the results of the regression models, three independent associated factors (TMD, FT4, Hb) and two indicators of LNM severity (Regions of LNM (RM), Quantitative Grading of LNM (QG)) were incorporated into the network model, as depicted in Fig. 4A. Consistent with the regression models, TMD exhibited a positive correlation with both RM and QG, while Hb and FT4 were negatively correlated with RM and QG. However, with regard to edge weights, the edge weights between TMD and RM, as well as TMD and QG, were more substantial compared to the edge weights between the other two associated factors and RM and QG. Furthermore, concerning the internal associations among the associated factors, the only negative correlation was observed between TMD and FT4, whereas the remaining edges exhibited positive correlations. The detailed edge weight matrix is provided in the Table S3.

The results of the community clustering are presented in Fig. 4B. The Walktrap algorithm identified two communities: one comprising TMD, RM, and QG, and the other comprising FT4 and Hb. The community clustering results suggest that, despite all being independent associated factors, the association between TMD and both RM and QG may be closer than the association between FT4 and Hb with RM and QG.

The evaluation of edge weight accuracy revealed that the 95% confidence intervals produced by the non-parametric bootstrap tests were of average width. Additionally, the analysis of edge weight differences showed that the edge weights were statistically robust. Further details can be found in Figure S1-2.

#### Discussion

To the best of our knowledge, this study is the first to employ both regression models and network analysis—two reliable data-driven approaches—to thoroughly investigate LNM in patients with coexistent PTC and HT. Not only did this study construct and externally validate three predictive models for LNM in patients with coexistent PTC and HT, but it also delved into the complex interrelations of the severity of LNM and its risk factors.

We identified four key characteristics associated with LNM in patients with HT and PTC: age  $\leq 47$  years, calcifications, serum FT3  $> 4.825$  pmol/L, and TMD  $> 1.15$  cm. Consistent with previous studies, age, calcifications, and tumor size are confirmed independent risk factors for predicting LNM in patients with HT and PTC or PTC alone. Interestingly, we found that elevated FT3 levels, even within the normal range, increased the likelihood of LNM.

Few studies have analyzed the relationship between thyroid hormones and LNM in HT combined with PTC. Wang et al.<sup>27</sup> found a positive correlation between FT3 levels and central LNM in PTC ( $P < 0.001$ ); Diessl et al.<sup>28</sup> suggested higher FT3 levels are associated with worse prognosis in advanced differentiated thyroid cancer. The relationship between elevated thyroid hormones and the proliferation and invasiveness of various solid tumors, including thyroid cancer, has been increasingly validated<sup>29</sup>. This study firstly demonstrated a positive correlation between FT3 levels and LNM in patients with both HT and PTC, although further verification in larger samples and exploration of the molecular basis are needed.

The regression model identified distinct independent risk factors in two subgroups of LNM severity. In the quantitative subgroup, TMD  $> 1.75$  cm and Hb  $< 121.5$  g/L are indicators of a higher number of LN metastases ( $> 5$  nodes); while in the regional subgroup, TMD  $> 1.85$  cm and serum FT4  $< 18.25$  pmol/L were associated with LLNM.

As expected, TMD emerged as an independent risk factor across subgroups, reinforcing its importance as a primary predictor of LNM in patients with both PTC and HT. In contrast to the commonly used tumor diameter threshold ( $> 10$  mm) for predicting LNM in patients with differentiated thyroid carcinoma (DTC)<sup>30</sup>, we propose a higher cutoff value specifically to assess whether patients with HT combined with PTC experience more severe lymph node metastases.

Additionally, our research proposes for the first time that lower Hb levels may serve as an independent risk factor for increased LNM. Although directly linking hemoglobin levels to LNM in TC remains underexplored,

Category	Total, n (%)	Quantity			Region		
		1–5 LNM, n (%)	>5 LNMs, n (%)	P	CLNM, n (%)	LLNM, n (%)	P
No. of patients	122	91 (74.6)	31 (25.4)		93 (76.2)	29 (23.8)	
Age (mean ± SD, years)	41.72 ± 11.02	39.12 ± 10.39	35.58 ± 10.30	0.103	38.26 ± 10.20	38.10 ± 11.36	0.945
<55	113 (92.6)	85 (93.4)	28(90.3)	0.691	88 (94.6)	25 (86.2)	0.214
≥ 55	9 (7.4)	6.6	3 (9.7)		5 (5.4)	4 (13.8)	
<b>Gender</b>							
male	17 (13.9)	15 (16.5)	2 (6.5)	0.233	13 (14)	4 (13.8)	1.000
Female	105 (86.1)	76 (83.5)	29 (93.5)		80 (86)	25 (86.2)	
<b>BRAF V600E mutation</b>							
Yes	90 (79.6)	70 (83.3)	20 (69)	0.098	68 (79.1)	22 (81.5)	0.786
No	23 (20.4)	14 (16.7)	9 (31)		18 (20.9)	5 (18.5)	
<b>TMD (mean ± SD, cm)</b>	1.21 ± 0.78	1.32 ± 0.82	1.88 ± 1.10	<b>0.003*</b>	1.33 ± 0.74	1.90 ± 1.29	<b>0.031*</b>
≤ 1 cm	52 (42.6)	44 (48.4)	8 (25.8)	<b>0.028*</b>	42 (45.2)	10 (34.5)	0.310
> 1 cm	70 (57.4)	47 (51.6)	23 (74.2)		51 (54.8)	19 (65.5)	
<b>Sum of tumor diameters (mean ± SD, cm)</b>	1.46 ± 0.95	1.58 ± 0.97	2.11 ± 1.13	<b>0.013*</b>	1.57 ± 0.91	2.17 ± 1.28	<b>0.026*</b>
<b>Multifocality</b>							
Yes	42 (34.4)	32 (35.2)	10 (32.3)	0.769	32 (34.4)	10 (34.5)	0.994
No	80 (65.6)	59 (64.8)	21 (67.7)		61 (65.6)	19 (65.5)	
<b>Tumor location (L/R/I/B)</b>							
Left	48 (39.3)	34 (37.4)	14 (45.2)	0.832	36 (38.7)	12 (41.4)	0.948
Right	47 (38.5)	36 (39.6)	11 (35.5)		36 (38.7)	11 (37.9)	
Isthmus	1 (0.8)	1 (1.1)	0(0)		1 (1,1)	0 (0)	
Bilateral	26 (21.3)	20 (22)	6 (19.4)		20 (21.5)	6 (20.7)	
<b>Calcification</b>							
Yes	105 (86.1)	78 (85.7)	27 (87.1)	1.000	80 (86)	25 (86.2)	1.000
No	17 (13.9)	13 (14.3)	4 (12.9)		13 (14)	4 (13.8)	
<b>Capsular invasion</b>							
Yes	24 (19.7)	14 (15.4)	10 (32.3)	<b>0.041*</b>	18 (19.4)	6 (20.7)	0.875
No	98 (80.3)	77 (84.6)	21 (67.7)		75 (80.6)	23 (79.3)	
<b>Extrathyroidal extension</b>							
Yes	4 (3.3)	1 (1.1)	3 (9.7)	0.050	2 (2.2)	2 (6.9)	0.239
No	118 (96.7)	90 (98.9)	28 (90.3)		91 (97.8)	27 (93.1)	
<b>Aspect ratio</b>							
≤ 1	36 (29.5)	30 (33)	6 (19.4)	0.151	28 (30.1)	8 (27.6)	0.795
> 1	86 (70.5)	61 (67)	25 (80.6)		65 (69.9)	21 (72.4)	
<b>Vascular invasion</b>							
Yes	6 (4.9)	3 (3.3)	3 (9.7)	0.156	3 (3.2)	3 (10.3)	0.145
No	116 (95.1)	88 (96.7)	28 (90.3)		90 (96.8)	26 (89.7)	
<b>TG (mean ± SD, ng/ml)</b>	18.58 ± 55.16	9.63 ± 18.97	29.53 ± 93.52	0.065	10.25 ± 21.23	28.34 ± 93.97	0.321
<b>TgAb (mean ± SD, IU/mL)</b>	593.33 ± 912.61	642.05 ± 1028.16	824.56 ± 1047.04	0.400	693.65 ± 1033.38	678.26 ± 1045.54	0.945
Normal	30 (24.6)	24 (26.4)	6 (19.4)	0.433	22 (23.7)	8 (27.6)	0.668
High	92 (75.4)	67 (73.6)	25 (80.6)		71 (76.3)	21 (72.4)	
<b>TPOAb (mean ± SD, IU/mL)</b>	181.61 ± 192.80	205.79 ± 214.10	127.23 ± 160.86	<b>0.037*</b>	200.60 ± 212.05	135.31 ± 168.36	0.140
Normal	44 (36.1)	29 (31.9)	15 (48.4)	0.098	30 (32.3)	14 (48.3)	0.117
High	78 (63.9)	62 (68.1)	16 (51.6)		63 (67.7)	15 (51.7)	
<b>FT3 (mean ± SD, pmol/L)</b>	4.89 ± 0.79	5.05 ± 0.79	4.96 ± 0.60	0.576	5.00 ± 0.75	5.09 ± 0.74	0.585
<b>FT4 (mean ± SD, pmol/L)</b>	16.43 ± 3.07	17.00 ± 3.03	15.70 ± 2.68	<b>0.037*</b>	16.97 ± 3.12	15.71 ± 2.35	<b>0.047*</b>
<b>TSH (mean ± SD, mIU/L)</b>	2.85 ± 1.96	2.58 ± 1.86	2.81 ± 2.10	0.564	2.61 ± 1.84	2.72 ± 2.17	0.788
<b>PTH (mean ± SD, pg/ml)</b>	41.86 ± 36.95	38.78 ± 16.62	35.15 ± 15.47	0.319	39.97 ± 16.92	31.56 ± 12.75	<b>0.020*</b>
<b>Leukocyte count (mean ± SD, 10<sup>9</sup>/L)</b>	5.78 ± 1.40	5.84 ± 1.33	5.79 ± 1.57	0.851	5.82 ± 1.36	5.85 ± 1.51	0.924
<b>Erythrocyte count (mean ± SD, 10<sup>12</sup>/L)</b>	4.87 ± 8.02	4.47 ± 0.50	4.24 ± 0.51	<b>0.027*</b>	4.44 ± 0.49	4.30 ± 0.57	0.175
<b>Hemoglobin (mean ± SD, g/L)</b>	129.59 ± 15.79	131.34 ± 14.51	124.52 ± 14.96	<b>0.027*</b>	130.39 ± 14.82	127.10 ± 14.99	0.301
<b>Platelet count (mean ± SD, 10<sup>9</sup>/L)</b>	215.27 ± 58.83	217.77 ± 57.19	203.68 ± 53.82	0.232	219.42 ± 57.93	197.41 ± 48.72	0.067
<b>Vitamin D3 (mean ± SD, nmol/L)</b>	20.48 ± 7.86	21.11 ± 8.04	19.24 ± 8.28	0.365	20.49 ± 8.55	20.76 ± 7.18	0.890
<b>Serum Ca<sup>2+</sup> (mean ± SD, mmol/L)</b>	2.32 ± 0.15	2.34 ± 0.11	2.28 ± 0.13	<b>0.033*</b>	2.33 ± 0.11	2.29 ± 0.12	<b>0.049*</b>

**Table 2.** Correlations analysis of the quantity or regions of LNM in patients diagnosed with lymph node metastasis. Note: Abbreviations: LNM, lymph node metastasis; CLNM, central lymph node metastasis; LLNM, lateral lymph node metastasis; TMD, tumor maximum diameter; Tumor location (L/R/I/B), tumor location (left/right/isthmus/bilateral); TG, thyroglobulin; TgAb, antithyroglobulin antibodies; TPOAb, thyroid peroxidase antibody; FT3, free triiodothyronine; FT4, free thyroxine; TSH, thyroid-stimulating hormone; PTH, parathyroid hormone. \* Means  $P < 0.05$ .

Indicators	B	OR value	95% CI		P
			lower	Upper	
<b>Model 1: Multivariate Logistic Analysis of LNM in Patients with Concurrent PTC and HT</b>					
Age (years)	-0.052	0.950	0.924	0.975	<0.001*
TMD (cm)	0.491	1.635	1.001	2.669	0.049*
Calcification	0.773	2.167	1.108	4.236	0.024*
FT3 (pmol/L)	0.370	1.448	1.018	2.06	0.039*
$B_0^{(1)}$	-1.530				
<b>Model 2: Multivariate Logistic Analysis for quantity of LNM</b>					
TMD (cm)	0.586	1.796	1.153	2.799	0.010*
Hemoglobin (g/L)	-0.034	0.967	0.938	0.997	0.029*
$B_0^{(2)}$	2.400				
<b>Model 3: Multivariate Logistic Analysis for regions of LNM</b>					
TMD (cm)	0.618	1.856	1.163	2.962	0.010*
FT4 (pmol/L)	-0.291	0.747	0.604	0.925	0.008*
$B_0^{(3)}$	2.626				

**Table 3.** Multivariate logistic analysis of LNM in patients with concurrent PTC and HT. Note: Abbreviations: LNM, lymph node metastasis; TMD, tumor maximum diameter; FT3, free triiodothyronine; FT4, free thyroxine. \* Means  $P < 0.05$ .

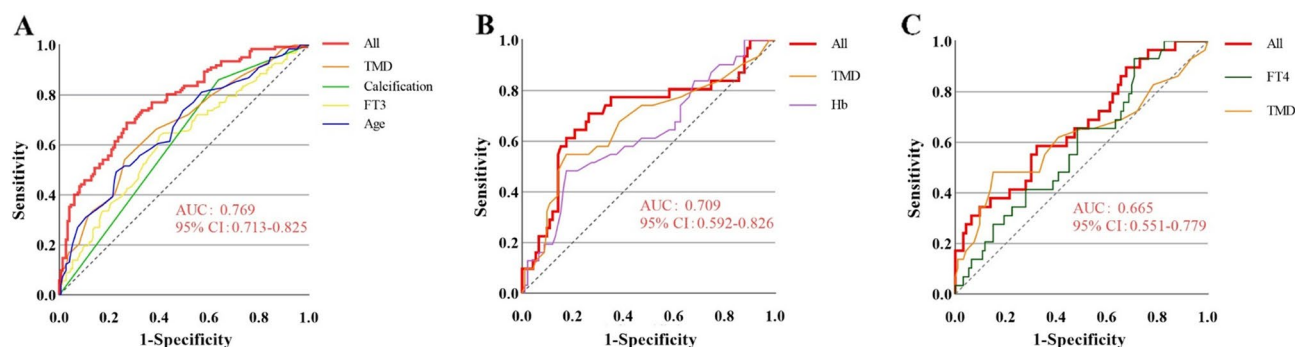


**Fig. 2.** ROC curve of multivariate logistic regression analysis in papillary thyroid cancer patients with Hashimoto thyroiditis. (A) ROC for presence or absence of lymph node metastasis (LNM); (B) ROC for the quantity of LNM; (C) ROC for the regions of LNM.



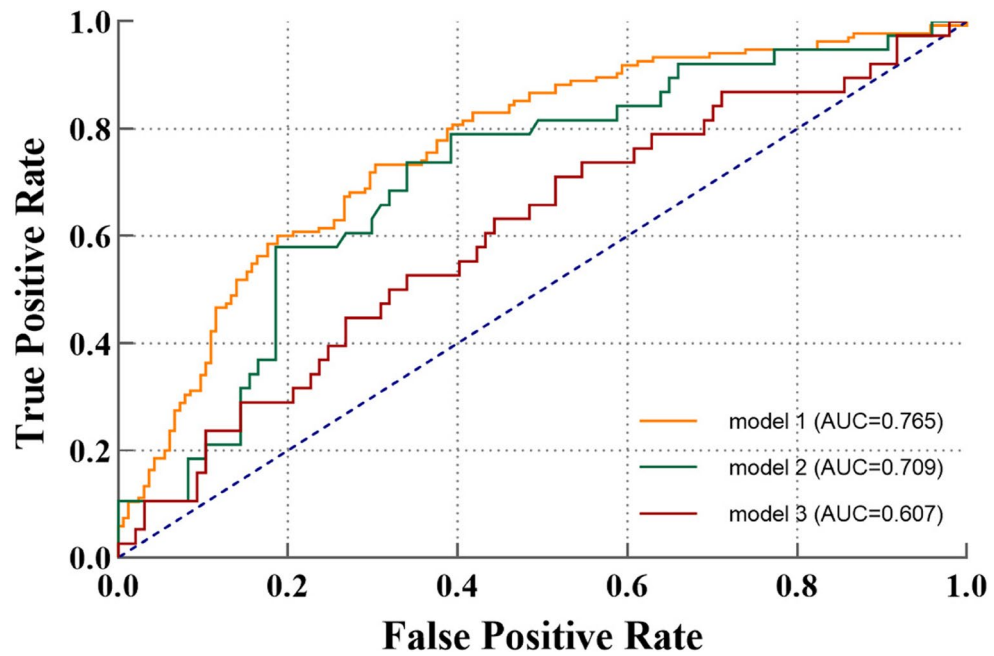


**Fig. 3.** ROC Curve for External Validation of Logistic Regression Model. Model 1 for the presence of LNM; Model 2 for the quantity of LNM; Model 3 for the regions of LNM.

the broader implications of low hemoglobin levels on cancer aggressiveness and outcomes are well-established in oncology literature<sup>31–33</sup>. Generally, reduced hemoglobin levels are correlated with increased malignancy severity and poorer prognoses across diverse cancer types. This association might suggest similar implications for TC, where systemic manifestations like anemia could indicate advanced or more aggressive disease states.

The finding that lower serum FT4 levels are linked to lateral LNM suggests a complex interplay of thyroid hormones affecting tumor behavior. Unlike FT3, lower FT4 appears to reduce LNM risk, potentially due to interactions within the hypothalamic-pituitary-thyroid (HPT) axis and the conversion of FT4 to the more active FT3. Typically, FT4 circulates predominantly and converts to FT3 locally. The HPT axis regulates thyroid hormones through feedforward and feedback mechanisms. Elevated T4 levels or reduced conversion to FT3 decreases TSH, which could influence LNM outcomes. Previous research has identified TSH as a risk factor for LNM in PTC<sup>34,35</sup>, although our study did not find significant TSH differences. Further clinical and molecular investigations are needed to understand these hormone interactions and their effects on LNM.

The results of the network analysis indicate that TMD exhibits a more intimate relationship with LNM compared to Hb or FT4. Furthermore, TMD is more closely associated with the quantity of LNM than with region of LNM. Tumors with larger TMD dimensions have an increased surface area for interstitial dissemination and metastatic spread, rendering them more likely to breach the thyroid capsule and invade adjacent tissues, consequently elevating the probability of metastasis to regional LN<sup>36,37</sup>. Furthermore, larger tumors may induce significant alterations in the local tissue microenvironment, including enhanced angiogenesis, the formation of an immunosuppressive milieu, and the activation of stromal cells, collectively facilitating cancer cell metastasis<sup>38,39</sup>. Although previous studies have identified potential associations between FT4, Hb, and LNM, these connections are more likely to be indirectly mediated through their effects on tumor cell biochemical metabolism<sup>40,41</sup>.

### Limitations

This study is subject to certain limitations. Firstly, as a single-center, case-control study, it only reflects the disease characteristics of patients from one institution, potentially introducing selection bias. Secondly, the data collection was not exhaustive regarding variables that might influence LNM in patients with HT combined with PTC, such as family history, behavioral factors, and body mass index (BMI). Therefore, future research should include multicenter, larger-scale cohort studies to validate and extend the findings presented herein.

### Conclusion

This study innovatively employs both regression models and network analysis to explore potential factors related to LNM in patients with coexisting PTC and HT, as well as the complex associations between these factors and the severity of LNM. The findings indicate that age, Hb, FT3, FT4, calcification, and TMD are all associated with LNM in patients with PTC and HT. Specifically, FT4 and Hb correlate with the regions and quantity of LNM, respectively, while TMD shows a significant association with both, exhibiting a stronger correlation than either FT4 or Hb. Overall, our results provide a theoretical basis for predicting preoperative LNM in patients with PTC and HT in future clinical practice.

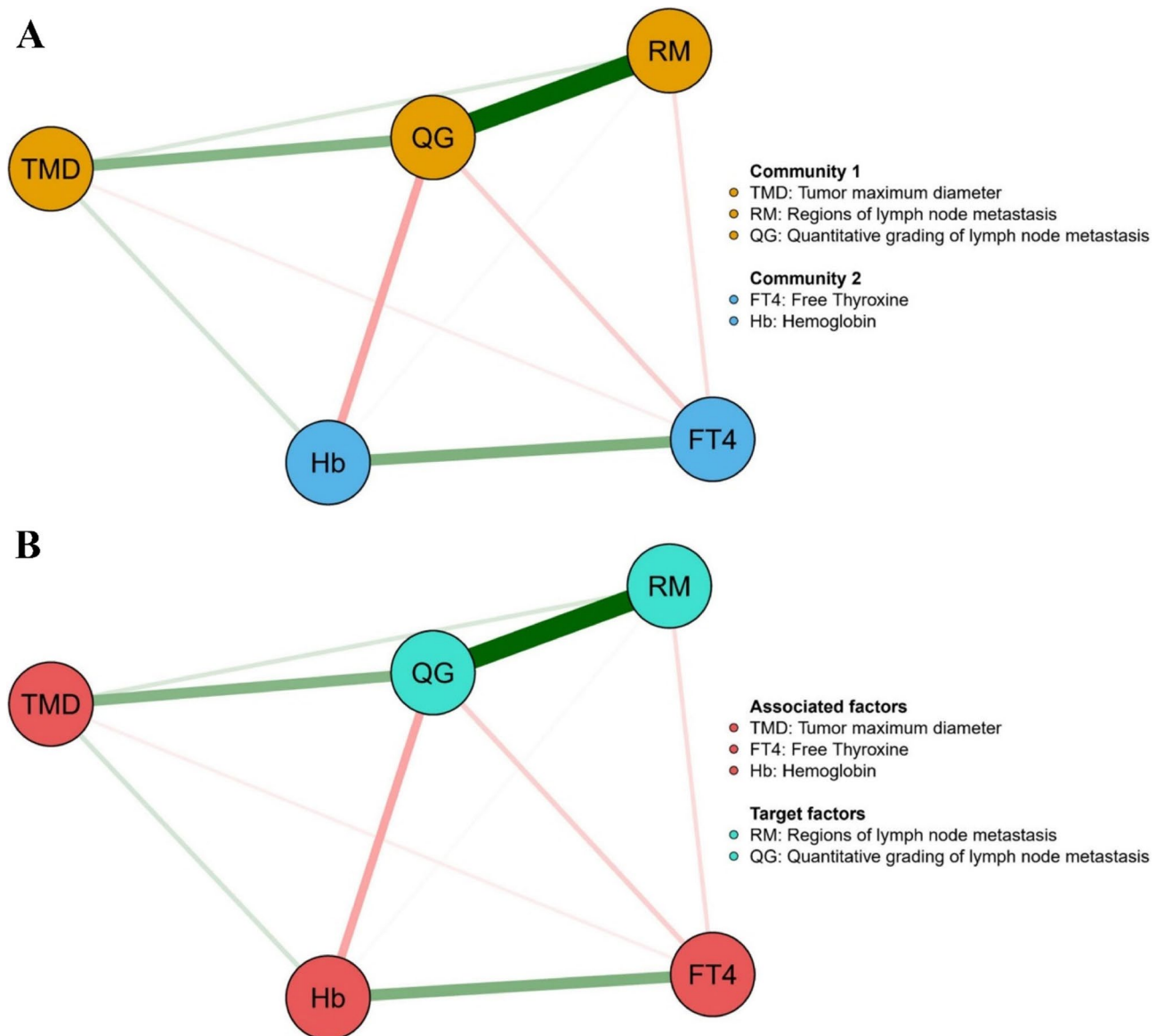


**Fig. 4.** Network structure and community clustering results of lymph node metastasis severity and associated factors. (A) Network structure of lymph node metastasis severity and associated factors. (B) Community clustering results of lymph node metastasis severity and associated factors.

### Data availability

The data that support the findings of this study are available on request from the corresponding author. The data are not publicly available due to privacy or ethical restrictions.

Received: 1 September 2024; Accepted: 29 October 2024

Published online: 11 November 2024

### References

- Janicki, L., Patel, A., Jendrzejewski, J. & Hellmann, A. Prevalence and Impact of BRAF mutation in patients with concomitant papillary thyroid carcinoma and Hashimoto's thyroiditis: a systematic review with meta-analysis. *Frontiers in endocrinology*. **14**, 1273498. <https://doi.org/10.3389/fendo.2023.1273498> (2023).
- Pizzato, M. et al. The epidemiological landscape of thyroid cancer worldwide: GLOBOCAN estimates for incidence and mortality rates in 2020. *The lancet Diabetes & endocrinology*. **10**(4), 264–272. [https://doi.org/10.1016/s2213-8587\(22\)00035-3](https://doi.org/10.1016/s2213-8587(22)00035-3) (2022).
- LeClair, K. et al. Evaluation of Gender Inequity in Thyroid Cancer Diagnosis: Differences by Sex in US Thyroid Cancer Incidence Compared With a Meta-analysis of Subclinical Thyroid Cancer Rates at Autopsy. *JAMA internal medicine*. **181**(10), 1351–1358. <https://doi.org/10.1001/jamainternmed.2021.4804> (2021).
- Haugen, B. R. et al. 2015 American Thyroid association management guidelines for adult patients with thyroid nodules and differentiated thyroid cancer: the american thyroid association management guidelines task force on thyroid nodules and differentiated thyroid cancer. *Thyroid J Am Thyroid Assoc*. **26**(1), 1–133. <https://doi.org/10.1089/thy.2015.0020> (2016).

5. Leboulleux, S. et al. Prognostic factors for persistent or recurrent disease of papillary thyroid carcinoma with neck lymph node metastases and/or tumor extension beyond the thyroid capsule at initial diagnosis. *The Journal of clinical endocrinology and metabolism*. **90**(10), 5723–9. <https://doi.org/10.1210/jc.2005-0285> (2005).
6. Min, Y. et al. Preoperatively Predicting the Central Lymph Node Metastasis for Papillary Thyroid Cancer Patients With Hashimoto's Thyroiditis. *Frontiers in endocrinology*. **12**, 713475. <https://doi.org/10.3389/fendo.2021.713475> (2021).
7. Xu, J. et al. Hashimoto's Thyroiditis: A "Double-Edged Sword" in Thyroid Carcinoma. *Front Endocrinol*. **13**, 801925. <https://doi.org/10.3389/fendo.2022.801925> (2022).
8. Ehlers, M. & Schott, M. Hashimoto's thyroiditis and papillary thyroid cancer: are they immunologically linked?. *Trends Endocrinol Metabol TEM*. **25**(12), 656–64. <https://doi.org/10.1016/j.tem.2014.09.001> (2014).
9. Zhang, Y., Dai, J., Wu, T., Yang, N. & Yin, Z. The study of the coexistence of Hashimoto's thyroiditis with papillary thyroid carcinoma. *J Cancer Res Clin Oncol*. **140**(6), 1021–6. <https://doi.org/10.1007/s00432-014-1629-z> (2014).
10. Tamimi, D. M. The association between chronic lymphocytic thyroiditis and thyroid tumors. *Int J Surg Pathol*. **10**(2), 141–6. <https://doi.org/10.1177/106689690201000207> (2002).
11. Tang, Q., Pan, W. & Peng, L. Association between Hashimoto thyroiditis and clinical outcomes of papillary thyroid carcinoma: A meta-analysis. *PLoS one*. **17**(6), e0269995. <https://doi.org/10.1371/journal.pone.0269995> (2022).
12. Wang, L. et al. Lymph node metastasis of papillary thyroid carcinoma in the context of Hashimoto's thyroiditis. *BMC Endocr Disord*. **22**(1), 12. <https://doi.org/10.1186/s12902-021-00923-2> (2022).
13. Xu, S. et al. Prevalence of Hashimoto Thyroiditis in Adults With Papillary Thyroid Cancer and Its Association With Cancer Recurrence and Outcomes. *JAMA Netw Open*. **4**(7), e2118526. <https://doi.org/10.1001/jamanetworkopen.2021.18526> (2021).
14. Luo, Q. W. et al. A novel tool for predicting the risk of central lymph node metastasis in patients with papillary thyroid microcarcinoma: a retrospective cohort study. *BMC Cancer*. **22**(1), 606. <https://doi.org/10.1186/s12885-022-09655-5> (2022).
15. Jara, S. M. et al. The relationship between chronic lymphocytic thyroiditis and central neck lymph node metastasis in North American patients with papillary thyroid carcinoma. *Surgery*. **154**(6), 1272–80. <https://doi.org/10.1016/j.surg.2013.07.021> (2013) (discussion 1280–2).
16. Ieni, A. et al. One-third of an Archival Series of Papillary Thyroid Cancer (Years 2007–2015) Has Coexistent Chronic Lymphocytic Thyroiditis, Which Is Associated with a More Favorable Tumor-Node-Metastasis Staging. *Front Endocrinol*. **8**, 337. <https://doi.org/10.3389/fendo.2017.00337> (2017).
17. Zeng, B. et al. Hashimoto's Thyroiditis Is Associated With Central Lymph Node Metastasis in Classical Papillary Thyroid Cancer: Analysis from a High-Volume Single-Center Experience. *Front Endocrinol*. **13**, 868606. <https://doi.org/10.3389/fendo.2022.868606> (2022).
18. Hussein, O. et al. Thyroid cancer associated with Hashimoto thyroiditis: similarities and differences in an endemic area. *J Egypt Natl Cancer Inst*. **32**(1), 7. <https://doi.org/10.1186/s43046-020-0017-9> (2020).
19. Zhang, L. et al. The clinical features of papillary thyroid cancer in Hashimoto's thyroiditis patients from an area with a high prevalence of Hashimoto's disease. *BMC Cancer*. **12**, 610. <https://doi.org/10.1186/1471-2407-12-610> (2012).
20. Vita, R., Ieni, A., Tuccari, G. & Benvenga, S. The increasing prevalence of chronic lymphocytic thyroiditis in papillary microcarcinoma. *Rev Endocrine Metabol Disord*. **19**(4), 301–309. <https://doi.org/10.1007/s11154-018-9474-z> (2018).
21. Kahan, B. C., Rushton, H., Morris, T. P. & Daniel, R. M. A comparison of methods to adjust for continuous covariates in the analysis of randomised trials. *BMC Med Res Methodol*. **16**, 42. <https://doi.org/10.1186/s12874-016-0141-3> (2016).
22. Friedman, J., Hastie, T. & Tibshirani, R. Sparse inverse covariance estimation with the graphical lasso. *Biostatistics (Oxford, England)*. **9**(3), 432–41. <https://doi.org/10.1093/biostatistics/kxm045> (2008).
23. Haslbeck, J. M. B. & Waldorp, L. J. How well do network models predict observations? On the importance of predictability in network models. *Behav Res Methods*. **50**(2), 853–861. <https://doi.org/10.3758/s13428-017-0910-x> (2018).
24. Lamartina, L. et al. 8th edition of the AJCC/TNM staging system of thyroid cancer: what to expect (ITCO#2). *Endocr Relat Cancer*. **25**(3), L7–111. <https://doi.org/10.1530/erc-17-0453> (2018).
25. Yang, Z., Algesheimer, R. & Tessone, C. J. A Comparative Analysis of Community Detection Algorithms on Artificial Networks. *Sci Rep*. **6**, 30750. <https://doi.org/10.1038/srep30750> (2016).
26. Epskamp, S., Borsboom, D. & Fried, E. I. Estimating psychological networks and their accuracy: A tutorial paper. *Behav Res Methods*. **50**(1), 195–212. <https://doi.org/10.3758/s13428-017-0862-1> (2018).
27. Wang, Z. et al. A Clinical Predictive Model of Central Lymph Node Metastases in Papillary Thyroid Carcinoma. *Front Endocrinol*. **13**, 856278. <https://doi.org/10.3389/fendo.2022.856278> (2022).
28. Diessl, S. et al. Impact of moderate vs stringent TSH suppression on survival in advanced differentiated thyroid carcinoma. *Clin Endocrinol*. **76**(4), 586–92. <https://doi.org/10.1111/j.1365-2265.2011.04272.x> (2012).
29. Lu, C., Zhu, X., Willingham, M. C. & Cheng, S. Y. Activation of tumor cell proliferation by thyroid hormone in a mouse model of follicular thyroid carcinoma. *Oncogene*. **31**(16), 2007–16. <https://doi.org/10.1038/onc.2011.390> (2012).
30. Mao, J. et al. Risk Factors for Lymph Node Metastasis in Papillary Thyroid Carcinoma: A Systematic Review and Meta-Analysis. *Front Endocrinol*. **11**, 265. <https://doi.org/10.3389/fendo.2020.00265> (2020).
31. Hoff, C. M. Importance of hemoglobin concentration and its modification for the outcome of head and neck cancer patients treated with radiotherapy. *Acta oncologica (Stockholm, Sweden)*. **51**(4), 419–32. <https://doi.org/10.3109/0284186x.2011.653438> (2012).
32. Farag, C. M., Antar, R., Akosman, S., Ng, M. & Whalen, M. J. What is hemoglobin, albumin, lymphocyte, platelet (HALP) score A comprehensive literature review of HALP's prognostic ability in different cancer types. *Oncotarget*. **14**, 153–172. <https://doi.org/10.18632/oncotarget.28367> (2023).
33. Mori, K. et al. Prognostic Value of Hemoglobin in Metastatic Hormone-sensitive Prostate Cancer: A Systematic Review and Meta-analysis. *Clin Genitourinary Cancer*. **18**(4), e402–e409. <https://doi.org/10.1016/j.clgc.2019.12.002> (2020).
34. Shahrokhi, M., Alsultan, M. & Kaban, Y. The relationship between papillary thyroid carcinoma and preoperative TSH level: A cross-sectional study from Syria. *Medicine*. **102**(28), e34283. <https://doi.org/10.1097/md.00000000000034283> (2023).
35. Yamamoto, M. et al. Active Surveillance Outcomes of Patients with Low-Risk Papillary Thyroid Microcarcinoma According to Levothyroxine Treatment Status. *Thyroid J Am Thyroid Assoc*. **33**(10), 1182–1189. <https://doi.org/10.1089/thy.2023.0046> (2023).
36. Ito, Y. et al. Prognostic factors for recurrence of papillary thyroid carcinoma in the lymph nodes, lung, and bone: analysis of 5,768 patients with average 10-year follow-up. *World J Surg*. **36**(6), 1274–8. <https://doi.org/10.1007/s00268-012-1423-5> (2012).
37. Edge, S. B. & Compton, C. C. The American Joint Committee on Cancer: the 7th edition of the AJCC cancer staging manual and the future of TNM. *Ann Surg Oncol*. **17**(6), 1471–4. <https://doi.org/10.1245/s10434-010-0985-4> (2010).
38. Mao, X. et al. Crosstalk between cancer-associated fibroblasts and immune cells in the tumor microenvironment: new findings and future perspectives. *Mol Cancer*. **20**(1), 131. <https://doi.org/10.1186/s12943-021-01428-1> (2021).
39. Jiang, X. et al. The role of microenvironment in tumor angiogenesis. *J Exp Clin Cancer Res*. **39**(1), 204. <https://doi.org/10.1186/s13046-020-01709-5> (2020).
40. Vaupel, P. & Mayer, A. Hypoxia in cancer: significance and impact on clinical outcome. *Cancer Metastasis Rev*. **26**(2), 225–39. <https://doi.org/10.1007/s10555-007-9055-1> (2007).
41. Fiore, E. & Vitti, P. Serum TSH and risk of papillary thyroid cancer in nodular thyroid disease. *J Clin Endocrinol Metabol*. **97**(4), 1134–45. <https://doi.org/10.1210/jc.2011-2735> (2012).

## Acknowledgements

The authors would like to thank all participants in this study.

## Authors' contributions

SC designed the study. LW, LZ, HT, BW, NL, NT, and PC acquired the data. LW, PC analyzed the data. LW wrote and revised the manuscript. All authors contributed to the article and approved the submitted version.

## Funding

This study was supported by grant 81902729 (S.C.) and 82300884 (N.T.) from the National Natural Science Foundation of China, grant 2020SK4003 (S.C.) from the Special Funding for the Construction of Innovative Provinces in Hunan, grant 2023JJ40990 (N.T.) from the Natural Science Foundation of Hunan Province, and grant 2021KFJ03 (S.C.) from the Project Program of National Clinical Research Center for Geriatric Disorders.

## Declarations

### Ethics approval and consent to participate

This study is part of the "Ultrasound and Clinical Big Data Research on Thyroid Diseases" project conducted by the Department of General Surgery (Hepatic and Thyroid Surgery) at Xiangya Hospital, Central South University. The project has been approved by the Ethics Committee of Xiangya Hospital, Central South University, with approval number 202211733. All methods were performed in accordance with the relevant guidelines and regulations, including the Declaration of Helsinki.

Written informed consent was obtained at the time of surgery for general use of clinical information in future studies. Given that minors typically do not possess the legal capacity and maturity to fully understand the nature, risks, and potential benefits of the study, the written informed consent for minors in this research will be confirmed by their parents or guardians to ensure the protection of their rights.

### Consent for publication

I would like to declare on behalf of my co-authors that our paper is new and neither the entire manuscript nor any part of its content has been published or has been accepted elsewhere. It is not in submission at any other journal.

All authors have approved of the final version of this manuscript.

### Competing interests

The authors declare no competing interests.

### Additional information

**Supplementary Information** The online version contains supplementary material available at <https://doi.org/10.1038/s41598-024-78179-8>.

**Correspondence** and requests for materials should be addressed to S.C.

**Reprints and permissions information** is available at [www.nature.com/reprints](http://www.nature.com/reprints).

**Publisher's note** Springer Nature remains neutral with regard to jurisdictional claims in published maps and institutional affiliations.

**Open Access** This article is licensed under a Creative Commons Attribution-NonCommercial-NoDerivatives 4.0 International License, which permits any non-commercial use, sharing, distribution and reproduction in any medium or format, as long as you give appropriate credit to the original author(s) and the source, provide a link to the Creative Commons licence, and indicate if you modified the licensed material. You do not have permission under this licence to share adapted material derived from this article or parts of it. The images or other third party material in this article are included in the article's Creative Commons licence, unless indicated otherwise in a credit line to the material. If material is not included in the article's Creative Commons licence and your intended use is not permitted by statutory regulation or exceeds the permitted use, you will need to obtain permission directly from the copyright holder. To view a copy of this licence, visit <http://creativecommons.org/licenses/by-nc-nd/4.0/>.

© The Author(s) 2024